

Role of Corrosion Products by the Sulfidation of AISI/SAE-1020 Steel in Heavy Crude Oil at High Temperatures

Javier Sanabria Cala^{*,a}, Carlos Mejía Miranda^a, Dionisio Laverde Cataño^a, Darío Y. Peña^{a,c}, Helmuth Sarmiento Klapper^b

^aGrupo de investigaciones en corrosión, Universidad Industrial de Santander, Bucaramanga, Colombia. Parque Tecnológico Guatiguara, Km 2 vía refugio, Piedecuesta, A.A. 681011, Colombia. Tel: +57 76 344000

^bCenter for Materials Research, Baker Hughes, Celle, Germany.

^cCenter for Materials and Nanosciences, Universidad Industrial de Santander.
sanabrialcalaj@gmail.com

The effect of temperature and exposure time on the formation of corrosion products on AISI/SAE-1020 steel was determined at typical service conditions of a transfer line that enters into an atmospheric distillation tower for processing heavy crude oil. The corrosion rate of the investigated material was determined in 12.2°API crude oil having 2.5%w/w of sulfur by weight loss measurements. The temperature and exposure time were varied in this study between 250 and 320°C, and between 36 and 504 hours, respectively. Corrosion products formed at the steel surface were characterized using scanning electron microscopy (SEM) combined with x-ray energy dispersive spectrometry (EDS) and x-ray diffraction (XRD). The obtained results have shown that both variables temperature and exposure time strongly influence the formation and stabilization of the corrosion products mainly iron sulfides formed at the steel surface being in contact with the high sulfur containing crude oil. After a period of stabilization, these corrosion products act as a physical barrier against corrosive species in the system thus reducing the corrosion rate of the investigated material.

1. Introduction

In the last years the development of upstream and downstream processes for extraction, transport and refining of heavy crudes oil (HCO) (Zheng et al., 2007), received significant attention within the oil and gas industry due to the remarkable quantities of recently proven reserves of HCO (Bota et al., 2010). One of the major challenges for refining HCOs relates to corrosion problems (Thompson et al., 2007), (Suleiman, 2015). The high sulfur (S) content present in HCOs (Kane and Cayard, 1999) in combination with the high temperatures necessary in refining processes affect significantly the integrity of the pipelines (Huang et al., 2012), and technical equipment involved in these processes (Kvarekval and Svenningsen, 2015). Corrosion and the subsequently formation of scales are the main degradation mechanisms of carbon steels used as manufacturing materials in refineries (Smith, 2015). Sulfidation at high temperatures (>232°C) (Serna, 2003), is one of the most common corrosion phenomena in refinery equipment (Zheng et al., 2015). This process is generated by the thermal breakdown of S to hydrogen sulfide (H₂S) that occurs at high temperatures. Hydrogen sulfide might become highly corrosive depending upon operating conditions (Alizadeh and Bordbar, 2013). However, it can also have some beneficial effect, due to the fact that corrosion products consisting in FeS compounds such as pyrite, troilite and mackinawite formed at carbon steel surfaces in contact with H₂S can act as a protective layer (Sanabria et al., 2014), (Bai et al., 2014). On the other hand, corrosion products containing FeS compounds might be removed due to high velocity flow of the liquid phase (Zheng et al., 2015). Therefore, sulfidation phenomena in refining facilities depend upon factors such as temperature, the S-content in the HCO, flow velocity and, obviously, the exposure time (Qi et al., 2014). The formation of corrosion products under conditions mimicking refining operations have been reported in the past (Sun et al., 2012). However, detailed information regarding the morphology and chemical composition of corrosion products formed at these conditions depending upon temperature and exposure time is not available (Yameng et al., 2012). In this study the influence of temperature and exposure time on the formation of FeS layers

formed on AISI/SAE-1020 steel was evaluated at the conditions observed during refining a HCO with high S content was evaluated. The corrosion rate of the material was determined by weight loss measurements and the formed corrosion products were characterized to establish the present phases and their morphology.

2. Methodology

The specimens used in this study were machined from AISI/SAE-1020 steel to obtain a rectangular shape with dimensions of 76 mm by 12.6 mm by 1.5 mm (length x high x width). The chemical composition of the studied material was determined by optical emission spectrometry according to ASTM E415 Standard and is included in Table 1.

Table 1. Chemical composition of the investigated AISI/SAE-1020 steel in wt. %

C	Cr	Mn	Ni	P	Si	S
0.201	0.032	0.665	< 0.0050	0.014	0.192	< 0.150

Prior to the experiments the surface of the specimens was mechanically ground using silicon carbide papers starting with grit 240 and subsequently polished up to 0.05 μm roughness according to ASTM G1-03 Standard. After surface preparation the gravimetric coupons were rinsed with deionized water and degreased with acetone in an ultrasonic bath. The experiments were conducted at three different temperatures: 250, 285 and 320°C. Each experimental condition was evaluated by a set of samples consisting in four gravimetric coupons. The set of samples was placed in the specimen holder of a dynamic autoclave. The tests were carried out at a stirring rate of 100 rpm in 1 liter of 12.2°API oil having 2.5% w/w of sulfur and density of 0.98 g/mL measured at 15°C. The content of dissolved oxygen in the HCO was reduced by means of purging the HCO one hour prior to testing with a constant flow of high purity analytical nitrogen. The specimens were evaluated after exposure times of 36, 48, 60, 72, 84, 96, 168, 360 and 504 hours in separate experiments. Once the targeted exposure time was completed, the set of samples were taken out of the autoclave, cleaned and weighted using an electronic balance with an accuracy of ± 0.001 g, labeled and stored in a desiccator for subsequent surface analysis. The corrosion products were characterized by Scanning Electron Microscopy (SEM) combined with X-ray Energy Dispersive Spectrometry (EDS). In addition, X-Ray Diffraction (XRD) was conducted using a diffractometer D8 Discover™ by Bruker with DaVinci Geometry in flush beam mode. The specimens for XRD were mounted and adjusted on the Eulerian cradle platform of the equipment.

3. Results and discussion

Figure 1 shows the mass gain of AISI/SAE-1020 steel in 12.2°API oil having 2.5% w/w of S at all tested temperatures. The data shown in Figure 1 correspond to average values obtained from each set of four single specimens. The maximal standard deviation was ± 0.004 g. As shown in Figure 1 the mass gain of the carbon steel was characterized by a linear increase in the first 96 hours of exposure. The mass gain continued increasing with time. However, at exposure times longer than 96 hours a non-linear increase in the mass gain of the investigated steel was observed at all three temperatures. The mass gain increased with increasing temperature and the largest changes in weight were determined on samples tested at 320 °C.

The corrosion rate of the AISI/SAE-1020 steel was calculated using Equation (1) and assuming that the measured mass gain is representative for the amount of metallic substrate that reacts with the HCO.

$$CR = 3.45 * 10^6 * \frac{\Delta W}{S * \rho * t} \quad (1)$$

In Equation (1) CR corresponds to the corrosion rate of the material in mpy, ΔW is the mass gain in g, S is the exposed surface area of the specimen in cm^2 , ρ is the density of the material (7.86 g/cm^3); t is the exposure time in hours, and 3.45×10^6 corresponds to unit conversion constant. The calculated corrosion rates of the AISI/SAE-1020 steel in the high S-containing HCO over the time are shown in Figure 2. Three different behaviors have been identified over the entire exposure time. It has been determined that the corrosion rate of the material increases significantly in the first 48 hours. Within this period of time, the higher the temperature the higher the calculated corrosion rate of the AISI/SAE-1020 steel. A period of stabilization follows the initial rapid increase in the corrosion rate, and the time-to-reach this condition as well as the duration of the stabilization period depend upon temperature. The corrosion rate of the AISI/SAE-1020 steel stabilizes after 48 hours at 320°C, after 60 at 285°C, and after 72 hours at 250°C. After 84 hours the corrosion rate of the material decreases considerably at all temperatures. The corrosion rates determined between 36 and 504 hours of exposure were always the highest at 320°C and the lowest at 250°C.

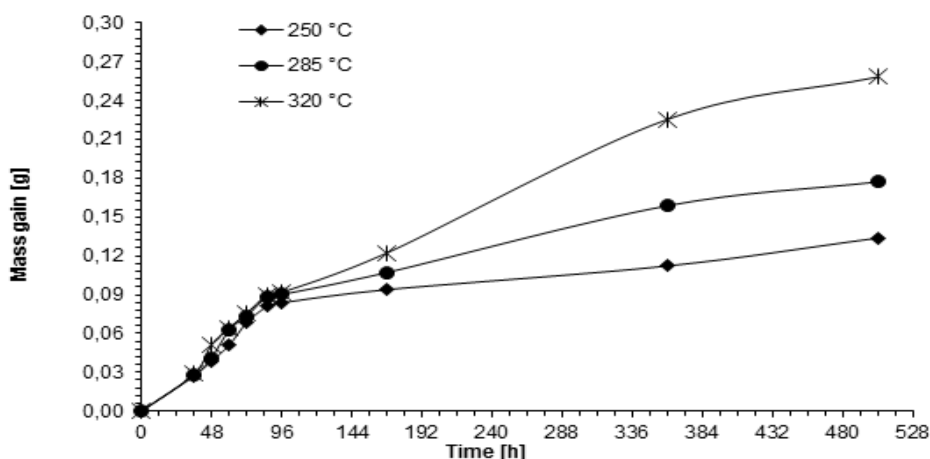


Figure 1. Mass gain of AISI/SAE-1020 steel in high-S HCO at different temperatures

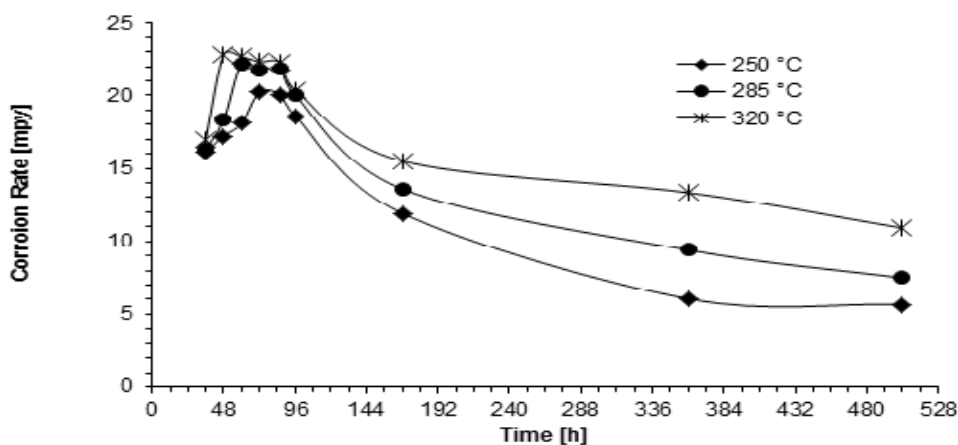


Figure 2. Corrosion rates of AISI/SAE-1020 steel in High-S HCO at different temperature

The morphology of the corrosion products formed on AISI/SAE-1020 steel surfaces at 320°C after exposure times of 96, 168, 360 and 504 hours was examined by SEM-EDS. These specimens were selected based on the fact that, as shown in Figure 2, the corrosion rate of the material dropped significantly in this range of exposure times. Figure 3 includes the micrographs of the corrosion products formed on AISI/SAE-1020 steel after different exposure times to the HCO at 320°C. The SEM-micrographs shown in Figures 3A, 3B, 3C and 3E document the increase in the grain size of the corrosion products formed on the steel surface with the exposure time. The average grain size changed from 466 nm after 96 hours to 621 nm after 168 hours and reached 2.2 μm after 360 hours. It has been also observed that the degree of crystallinity of the corrosion products changed with the exposure time. After 360 hours the formation of a bilayer of corrosion products at the surface was confirmed (Figure 3D). The typical grain sizes range from 3.4 μm in the upper layer up to 8.5 μm in the lower layer. The chemical characterization of the bilayer formed after 360 hours of exposure at 320°C by EDS indicates an increased sulfur content of 38% w/w at the upper layer compared to 28% w/w in the lower layer. It was also found that the bilayer was replaced after 504 hours by a compact and homogeneous single layer of corrosion products having an S-content of 32% w/w at 320°C.

The analysis of the corrosion products formed at the surface of the AISI/SAE-1020 steel exposed to a temperature of 320°C and after exposure times of 96, 168, 360 and 504 hours by XRD confirmed that the crystalline phases that are present with greater intensity correspond to sulfur compounds. The determined phases are listed in Table 2.

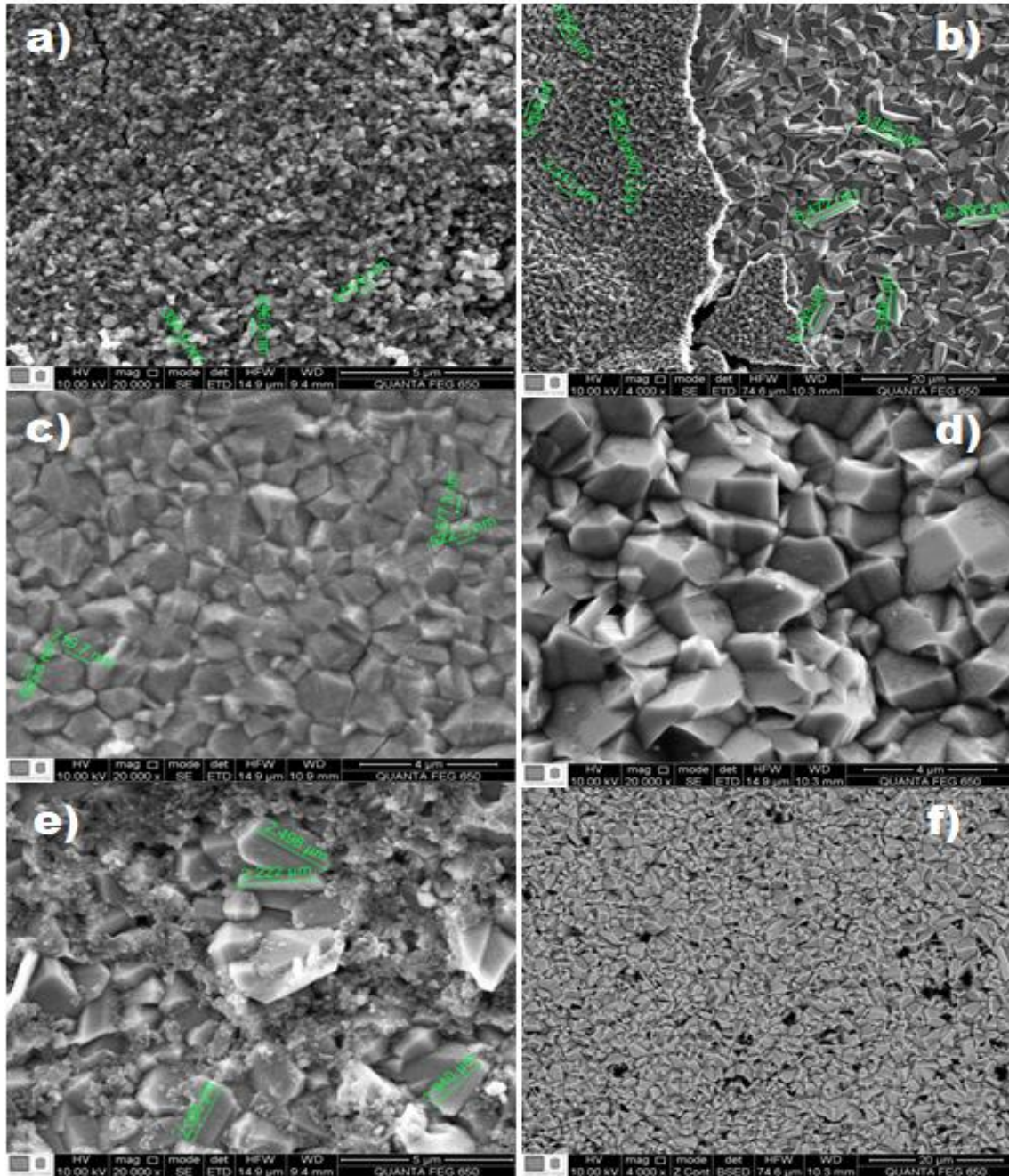


Figure 3. SEM-micrographs of corrosion products formed on AISI/SAE-1020 steel in HCO at 320°C after exposure times of A) 96 h, B) 168 h, C) and D) 360 h, E) and F) 504 h.

Table 2. S-Compounds determined on AISI/SAE 1020 Steel exposed to HCO at 320°C

Crystalline Phases	96 h	168 h	360 h	504 h
(Fe _{1-x} S)	Pyrrhotite-6T	Pyrrhotite-6T	Pyrrhotite-6T	Pyrrhotite-6T
(FeS)	Iron sulfide	Iron sulfide	Iron sulfide	Iron sulfide
(FeS)	Troilite-2H	Troilite-2H	Troilite-2H	Troilite-2H
(Fe _{0.975} S)	Iron sulfide		Iron Sulfide	
(Fe _{1-x} S)	Pyrrhotite-4H			
Fe ₉ S ₁₀				Iron sulfide
(Fe _{0.94} S)			Troilite	

Cross-sectional samples were prepared to analyze the morphology of the corrosion products mainly iron sulfide compounds formed at the surface of the AISI/SAE-1020 steel after 504 hours of exposure to the HCO at 320°C. SEM analysis has shown that the metallic substrate is almost uniformly covered by a 2.273 μm thick and compact layer of corrosion products (Figure 4). EDS analysis confirmed that the S-content of the corrosion products formed after 504 hours corresponds to 6.4% w/w (Figure 4).

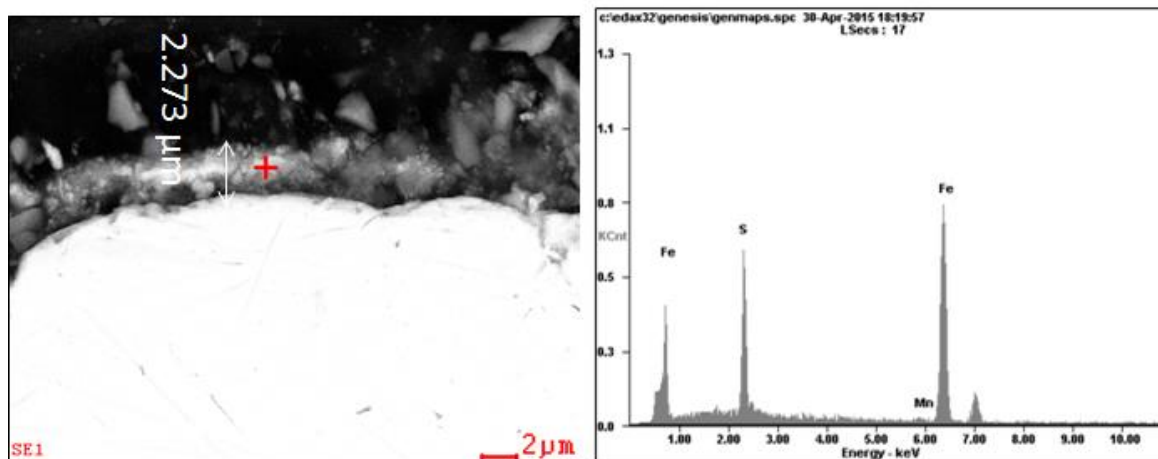


Figure 4. SEM-EDS of the Cross-Sectional products formed in AISI/SAE-1020 steel in HCO at 320°C and exposure time of 504 h.

Experimental results have shown that the corrosion rate of the AISI/SAE-1020 steel in the 2.5%w/w S-containing HCO exhibit three different regions over the exposure time considered in this study (Figure 2). The corrosion rate of the material reached values close to 16 mpy in the first 36 hours regardless the testing temperature. During the next 12 hours of exposure the corrosion rate continues increasing but in this period of time the increase in the corrosion rate of the material is directly depended upon the temperature. Apparently, the corrosion products formed in the first 48 hours of exposure are not stable enough to protect the material. At longer exposure times the corrosion rate shows a plateau at all temperatures. This plateau in the corrosion rate of the investigated material can be explained in terms of the stabilization of the corrosion products formed at the carbon steel surface. The time necessary to stabilize the corrosion products of the AISI/SAE-1020 steel depends strongly upon the temperature. The higher the temperature the faster the corrosion rate stabilizes. Also the period of stabilization in which the corrosion rate of the material does not change considerably longer with increasing temperature. This indicates that the formation of corrosion products at the steel surface is mainly driven by the thermal-breakdown of the S present in the HCO leading to the formation of H_2S . The corrosion behavior of the investigated material in the first 96 h of exposure can be explained in terms of two competing process. On one side, higher temperature supports the H_2S -formation reaction leading to higher corrosion rates. The more H_2S becomes available the higher the amount of substrate that reacts to corrosion products. On the other hand, the stabilization of the corrosion products formed at the steel surface is supported by temperature. Higher temperature leads to a faster stabilization of the corrosion rate but with higher values, as shown in Figure 2. At exposure times longer than 96 h a parabolic decrease in the corrosion rate of the material follows the initial rapid increase and the subsequently period of stabilization in the corrosion rate. The reduction in the corrosion rate after 96 h was irrespective of the temperature. Such behavior has been attributed to the stabilization of corrosion products mainly FeS-containing species at the metallic surface (Bai et al., 2014). In this study different corrosion products mainly iron sulfides with different stoichiometric ratios have been identified (Ma et al., 2000), (Rickard and Luther, 2007). Given their molecular complexity these compounds become indistinguishable from each other. The crystalline structure of the corrosion products formed on the AISI/SAE-1020 steel corresponding to irregular hexagons becomes thermodynamically stable after 96 hours of exposure, and thus favors its protective character. A similar behavior has been also seen in other materials exposed to similar corrosive environments. It is also known that minimal changes in operational conditions can lead to different morphologies of the FeS layers formed at steel surfaces (Sanabria et al., 2014). According to the experimental results obtained in this study, the crystalline corrosion products formed at the AISI/SAE-1020 steel surface after 96 hours of exposure to the HCO with high S-content at temperatures between 250 and 320°C reduce the corrosion rate around 35%.

4. Conclusions

The gravimetric tests that were conducted at temperatures similar to those present in the transfer lines for processing HCO with have shown a reduction in the corrosion rate of the AISI/SAE-1020 steel by exposure times longer than 96 in the temperature range between 250 and 320°C. Such behavior is due to the formation of a homogeneous and compact layer of FeS compounds at the material surface. Compact layers of corrosion products that consist mainly in pyrrhotite, troilite and iron sulfide formed at the surface of the AISI/SAE-1020 steel after 96 hours of exposure to HCO in the temperature range between 250 and 320°C. These layers have a protective character, thus lead to a reduction in the corrosion rate of the material. The characterization by SEM-EDS of the corrosion products formed on AISI/SAE-1020 steel in contact with the investigated HCO confirmed that the grain size of the corrosion products mainly FeS changed with increasing the exposure time. It was also established that the corrosion products having initially irregular morphology with no defined.

References

- Alizadeh M., Bordbar S., 2013, The influence of microstructure on the protective properties of the corrosion product layer generated on the welded API X70 steel in chloride solution, *Corros. Sci.* 70, 170–179.
- ASTM Standard E415, 2011, Standard Test Method for Analysis of Carbon and Low-Alloy Steel by Spark Atomic Emission (West Conshohocken, PA: ASTM International).
- ASTM Standard G1-03, 2011, Standard Practice for Preparing, Cleaning, and Evaluating Corrosion Test Specimens” (West Conshohocken, PA: ASTM International).
- Bai P., Zheng S., Zhao H., Ding Y., Wu J., Chen C., 2014, Investigations of the diverse corrosion products on steel in a hydrogen sulfide environment, *Corros. Sci.* 87, 397–406.
- Bota G., Qu D., Nescic S., 2010, Naphthenic acid corrosion of mild steel in the presence of sulfide scales formed in crude oil fractions at high temperature, *CORROSION/2010*, paper no 10353, (Houston, TX: NACE).
- Huang B, Yin W, Sang D, Jiang Z. 2012, Synergy effect of naphthenic acid corrosion and sulfur corrosion in crude oil distillation unit. *Appl. Surf. Sci.* 259, 664–670.
- Kane R.D., Cayard M.S., 1999, NACE Committee Report 8X294: Review of Published Literature on Wet H₂S Cracking, *CORROSION/1999*, paper no 420, (Houston, TX: NACE).
- Kvarekval J., Svenningsen G., 2015, Effect of High H₂S Partial Pressures on Localized Corrosion of Carbon Steel, *CORROSION/2015*, paper no 5720, (Houston, TX: NACE).
- Ma H.Y., Cheng X.L., Li G.Q., Chen S.H., Quan Z.L., Zhao S.Y., Niu L., 2000, The influence of hydrogen sulfide on corrosion of iron under different conditions, *Corros. Sci.* 42, 1669–1683.
- Qi Y., Luo H, Zheng S., Chen C., Lv Z., Xiong M. 2014, Effect of temperature on the corrosion behavior of carbon steel in hydrogen sulphide environments, *Int. J. Electrochem. Sci.* 9, 2101-2112.
- Rickard D., Luther G.W., 2007, Chemistry of iron sulfides, *Chem. Rev.* 107, 514–562.
- Sanabria J., Laverde D., Vásquez C., Blanco C., Quiroga H., 2014, Evaluación del efecto del contenido de azufre en la velocidad de corrosión del acero grado A335-P9 en un crudo pesado, *Rev. Ion* vol.27, 35-41.
- Serna J., 2003, Oxidación, carburación y sulfidación de aleaciones ferríticas Fe-9Cr-1Mo modificadas en ambientes con hidrocarburos a temperaturas entre 550 y 750°C. Tesis de Doctorado. Universidad Industrial de Santander, Bucaramanga, Colombia.
- Suleiman M., 2015, Sulphur species corrosivity in refinery feed stock, *Solid. State. Phenom.* 227, 213-216
- Smith S., 2015, Current Understanding of Corrosion Mechanisms Due to H₂S in Oil and Gas Production Environments, *CORROSION/2015*, paper no 5485, (Houston, TX: NACE).
- Sun H., Fang H., Hudgins D., 2012, Investigation of Effects of Iron Sulfide on Corrosion and Inhibition of Carbon Steel in H₂S Containing Conditions, *CORROSION/2012*, paper no 1651, (Houston, TX: NACE).
- Thompson N., Yunovich M., Dunmire D., 2007, Cost of corrosion and corrosion maintenance strategies, *Corros. Rev.* 25, 247-262.
- Yameng Q., Luo H., Zheng S., Chen C., Wang D., 2012, Effect of immersion time on the hydrogen content and tensile properties of A350LF2 steel exposed to hydrogen sulphide environments, *Corros. Sci.* 69, 164-174.
- Zheng Q., Jing H., Yao Z., 2005, High temperature naphthenic acid corrosion and sulphidic corrosion of Q235 and 5Cr1/2Mo steels in synthetic refining media, *Corros. Sci.* 48, 1960-1985.
- Zheng Y., Ning J., Brown B., Young D., Nescic S., 2015, Mechanistic study of the effect of iron sulfide layers on hydrogen sulfide corrosion of carbon steel, *CORROSION/2015*, paper no 5933, (Houston, TX: NACE).